

Article

# Debris Flow Generation Based on Critical Discharge: A Case Study of Xiongmao Catchment, Southwestern China

Lingfeng Gong<sup>1</sup>, Chuan Tang<sup>1,\*</sup>, Jiang Xiong<sup>1</sup>, Ning Li<sup>1</sup>

<sup>1</sup> State Key Laboratory of Geohazard Prevention and Geoenvironment Protection, Chengdu University of Technology, Chengdu 610059, China; glf025@163.com (L.F.G.); 2029476606@qq.com (J.X.); 790626903@qq.com (N.L.)

\* Correspondence: tangc707@gmail.com; Tel.: +86-28-8407-8948

**Abstract:** A debris flows generation related to a poorly sorted mixture of soil, catchment topography and rainfall characteristic. Runoff of some depth on valley resulting from intensive rainfall can incur the sediments movement of beds or adjacent banks. The fluid flow in channel affected by rainfall parameters combinations, such as duration, intensity, cumulative rainfall, etc., is the key factor for debris movement. In this paper, the rainfall characteristics and occurrence conditions of debris flow in Xiongmao gully on July, 26th, 2016, have been explored, combined with field survey and indoor simulation experiment on the collected critical discharge parameters of debris movement. Further, debris distribution and the critical discharge characteristics have been analysed, by means of investigation on the catchment topography and occurrence cause of the debris flow, analysis of the critical discharge parameters on which the channel debris began to move, and K value clustering analysis method to characterize the rainfall pattern of the studied area, the discharge calculation of debris flow occurring in different rainfall patterns. The results have shown that, for the debris flow occurrence in Xiongmao gully, the debris initiation on the middle reaches of the gully provide the majority of solid particles for the disaster on July, 26th, 2016, and the upstream confluent provided catchment. Based on the relationship obtained from laboratory test, in which the calculated critical discharge was  $43.8\text{m}^3/\text{s}$ , less than the peak discharge ( $Q_c = 66.7\text{m}^3/\text{s}$ ), calculated by morphological method. In addition, it has been indicated that the dominated rainfall patterns of the studied area are first-quartile and second-quartile, that is, the rainfall is primarily at earlier or middle to preliminary stage of this time rainfall event. The critical discharge for the occurrence of debris flow on July, 26th was achieved 20a rainfall frequency, the larger runoff volume generated on shorten heavily rainfall. Based on individuality characteristics, such as distributed hydrological analysis, critical discharge and rainfall pattern of debris flow, the forewarning could be more efficient.

**Keywords:** debris flow initiation; critical discharge; rainfall patterns; distributed hydrological

---

## 1. Introduction

Some debris flows initiated from mixture soil with a high enough water flow in southwestern China. Methods of the debris flow initiation include field observation [1-3], laboratory flume experiment [4-6], and data statistics, theoretical derivation [7-9]. Debris flow occurs frequently in catchments which have well-developed main channels and tributary gullies. The evolvement of debris flow after earthquake is featured with increased coarse matters and frictional resistance, which decreased occurrence frequency, and increased

difficulty on debris flow identification or prediction. According to the characteristics of debris flows, Tang et al (2008)[10] pointed out that the critical precipitation and initial discharge can be taken as an indicators for the initiation of debris flows. The discharge per unit width ( $\text{m}^3/\text{s}\cdot\text{m}$ ) was taken as the available indicator of debris flow initiation[2,7,9], due to the fact the discharge in combination with parameters like debris grain size, slope angle, sediment concentration can be obtained and applied to scientific research, prediction and practice.

Some flume experiment simulations of runoff discharge designed by experiment [6] taking gully bed gradient and average particle size into consideration. Coe et al (2008) [2]verified the accuracy of the critical discharge of overland runoff based on the field observation data. But they are different from the source of Wenchuan earthquake area obviously; and deposit heterogeneity should be considered when the critical discharge of debris flow is computed. That is the same average grain size or fine particle only under 10mm in flume test do have limitation on Wenchuan earthquake area. High concentration of runoff in upstream result in the sediment mobilization in midstream, similarly reproduce the laboratory tests in [11]. The critical discharge can be simulated in serial test and calculated with its relationships avoiding analyze hydrodynamic force using the size and slope. The parameter of critical discharge could be an effective criterion in channel sediment instability.

According to the distributed hydrological model, such as HEC-HMS [12], inHM [13], the surface or subsurface hydrologic responses could be simulated. With the surface runoff discharge, two methods (1) Manning's formula [14-16] and (2) by Shen's method [17] can be used to calculate the discharge of debris flow. Then the hydrological response analysis on critical precipitation and discharge became more available, meanwhile the debris flow discharge prediction can be feasibly. Rainfall, as an important factor formulized as I-D curve for debris flow initiation, has been frequently used [2,18-20]. The different rainfall patterns had shown on Wenchuan earthquake area [19], the runoff coefficient and peak discharge of an instantaneous heavy rainfall can be 5 to 6 times higher compared with an uniform rainfall intensity [21]. As a potential factors of initiation, the same scales of cumulative rainfall may lead to different water discharge when rainfall pattern is different.

For rainfall patterns estimation, Huff (1967; 1990) [22,23]firstly divided the precipitation process into four phases, and NOAA (the National Oceanic and Atmospheric Administration) published the Huff curve around America [24], while Azli et al (2010)[25], Domen et al (2016) [26] studied the temporal characteristic of rainfall around China, Peninsular Malaysia and Slovenia based on Huff curve. To reveal how confluence in the catchment changed with different rainfall patterns, the rainfall data used in this paper were from three rainfall stations located in Longmen Mountain (Table 1), and meteorolog of these stations are similar with that of a station in the Yuzi River in Yingxiu.

The paper is aimed to obtain the rainfall patterns statistically. The corresponding runoff discharge and debris flow discharge based on distributed hydrological modeling, field survey and developed relationship. Then a further prediction on rainfall threshold combined with rainfall patterns has been made. Direct survey of the debris flow on July, 26th, 2016 on Xiongmao ravine and 165 effective rainfall have been collected.

## 2. Study area

The Xiongmao gully, located at Wolong nature reserves, southwest of Wolong, Wenchuan county, Sichuan Province, was the primary tributary on the right bank of Yuzi river. The average longitudinal length of the gully is 8.8km, average width is 3.4km, average longitudinal grade is 169.9‰, and the catchment area is 23.6km<sup>2</sup>. Additionally, the highest elevation located at the southwest outlet of the gully is 3600m; the lowest one at the junction between the outlet and the Yuzi River is 2105m. The upstream catchment contains 6 branches with lengths from 0.9 to 2.4km and longitudinal gradients from 15 to 35% (Figure 1, 2).

The catchment consists of carbonaceous phyllites, sandy phyllites, slates and crystalline limestones. The upstream topography of the gully has an “U”-shape and the vegetation consists mainly of shrubs; while the downstream valley has more or less a “V”-shape, with steep slopes on both sides and well-developed cliffs with the gradients of  $50^{\circ}\sim 70^{\circ}$ . The channel sediment (red areas in Figure 2) on midstream, and collapse accumulation (yellow areas in Figure 2) on upstream compose the majority solid material. And midstream erosion extremely on red areas, hence, main initiation occurred along the 6# tributary and 5# tributary.

Debris flows broke out in the Xiongmao gully in 1995, 1998 and May 2004, respectively, destroying large areas of agricultural land, but no casualties were reported. The Wenchuan earthquake triggered many landslides, producing a lot of debris deposits in the upstream catchment, which provided abundant source material for debris flows.

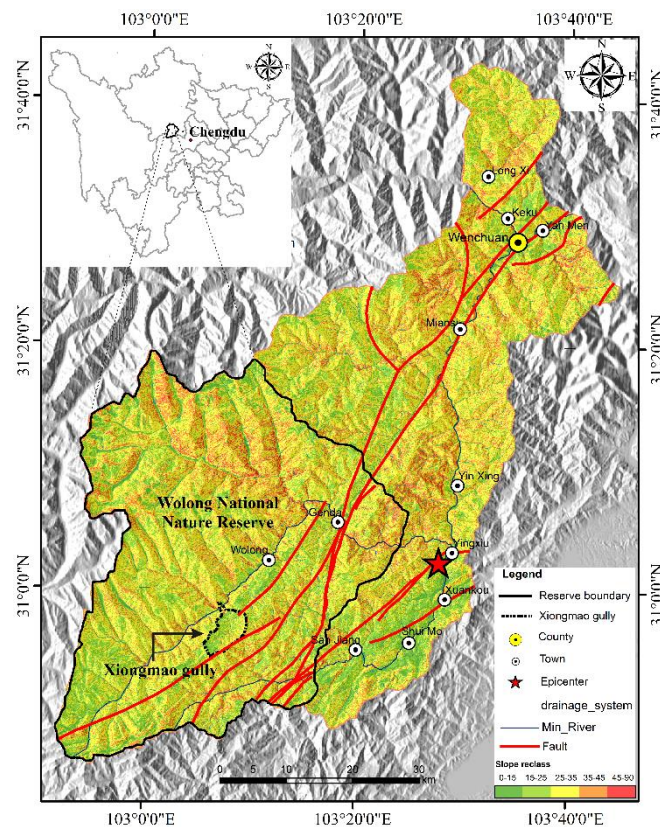


**Figure 1.** Map of the Xiongmao gully, located in the Wolong National Nature Panda Reserve.

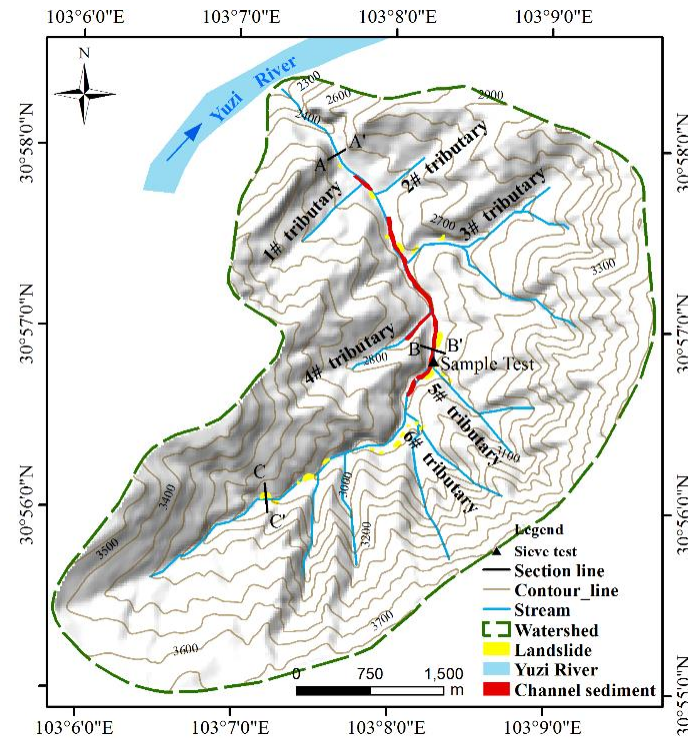


**Figure 2.** Xiongmao catchment topography and distribution of source materials in which the black lines are the investigated cross sections and the black triangle with numbers are the sampling points for the physical tests.

On July 26<sup>th</sup> 2016, a sudden rainstorm with cumulative rainfall about 70mm during 14:00~16:00. in Wolong increased the water discharge of Yuzi river significantly, and till 16:00, a debris flow occurred in the Xiongmao gully, and the debris rushed out flooded roads, blocked the tributary rivers in the catchment and the Yuzi river, generating tremendous economic damage to the local people and infrastructures (Figure 3). According to the Manual of Flood in Small Watershed of Sichuan Province, the rainfall within 24h with frequencies of 100a, 50a, 20a, 10a in the Xiongmao gully were 211.5mm, 190.8mm, 162.0mm, and 139.5mm, and the rainfall within 6h were 127.4mm, 113.7mm, 94.6mm, and 79.4mm respectively.

The longitudinal profile on Xiongmao gully revealed that the whole gully gradually became slow from the upstream longitudinal gradient, 207‰, then the mean longitudinal gradient of the original area was just 106‰-144‰. Especially, the gently longitudinal gradient of the original area made the debris easily be deposited and decreased debris flow velocity. While at the downstream transition area, the longitudinal gradient became abrupt, and could reach 450‰ at maximum, which was helpful to outrush of debris flow till to Yuzi River (Figure 4).



**Figure 3.** Photo of the scene of the debris flow on July, 26th, 2016: (a) the outbreak of the debris flow before blocking of the main river: (b) emergency drainage of the debris flow which has dammed the river.

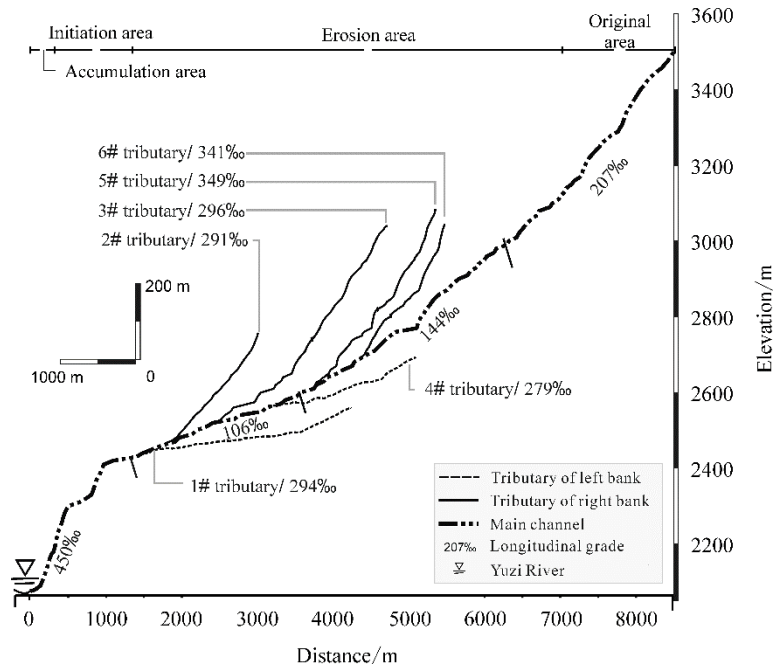


**Figure 4.** Longitudinal slope line of Xiongmao gully and longitudinal gradient diagram

The Xiongmao gully could be divided into a source area, a transition and an accumulation zone. Figure 5a, 5b show the upper and lower part of the transition zone, Figure 5c shows a cross section through the source area, while Figure 5d, 5e, 5f are photos of transition zone with deep gully, sediment initiation area, and flood flow area respectively.

The gully length of transition zone is about 0.83km, and the average longitudinal grade is about 38% with a maximum of 45%. The gully has in this section a “V” shape character with a width of 3 to 8m. The channel bed is eroded seriously, with on both sides were steep rock slopes with practically no landslides (Figure 5a, 5d).

The topography of source area has a U-shape character with bank slopes on both sides and abundant unconsolidated material. Most of the slope eroded as slightly bank cutting (Figure 5c, 5f). The upstream valley is covered by a thin layer of weathered deposits and dense vegetation. This region consists bare rock slopes and therefore, this area can generate a lot of run-off water for debris flow initiation.

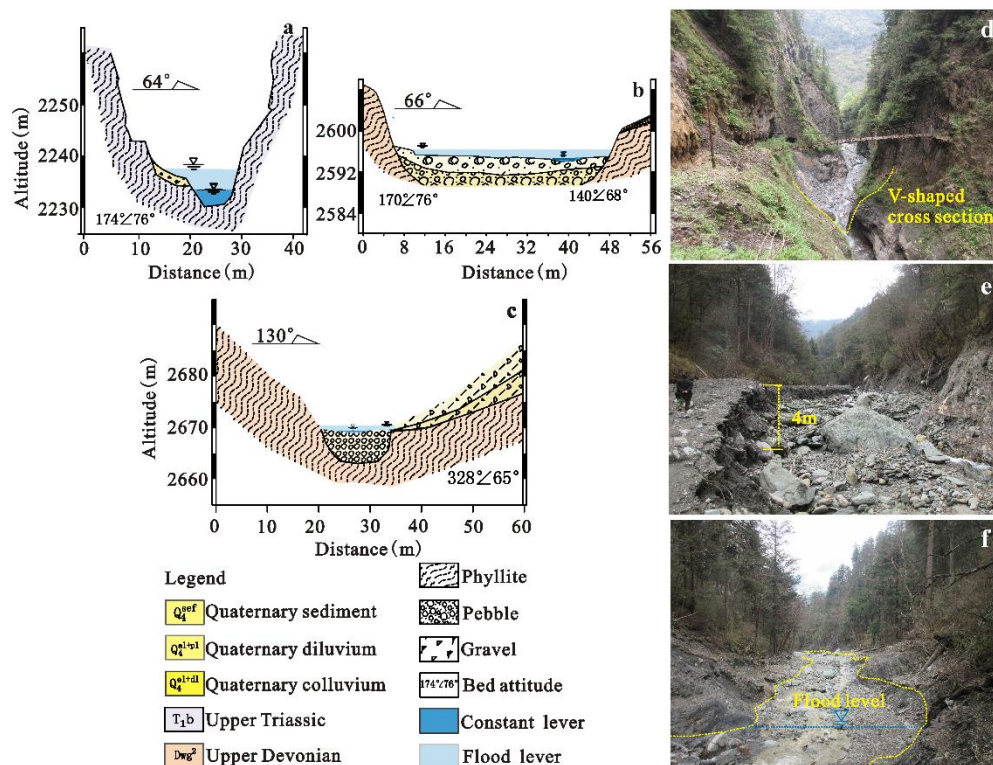


**Figure 5.** Morphological characteristic of the in Xiongmao gully. (a), (d) a crosssection of transition zone in which the gully is narrow with exposed bed rock slopes: (b), (e) a typical crosssection of the accumulation zone in which the gully is wide with large amounts of solid material: (c) the erosion of slope deposits in the upstream area: (f) nearly no solid materials in the upstream gully.

It was known from the source distribution of debris flow in Figure 2 and investigation in Figure 5 that hyper-concentration flow generated from the upstream of Xiongmao gully after sufficient confluence flow, and the channel deposits eroded by the runoff between Junction 2 and 3. Therefore, it was necessary to calculate the critical discharge at this location.

### 3. Methods

Through the laboratory flume experiment relationship, the natural channel critical discharge of debris flow initiation can be investigated based on source distribution, morphology, topography, and grain composition test. The rainfall characteristics of Longmen mountain area are explored using the dynamic K-value clustering analysis method. Based on HEC-HMS, the hydrological characteristics of catchment are analyzed under different frequencies and rainfall patterns to predict the critical discharges, giving significant reference for the research on rainfall and critical discharge of debris flow in earthquake area.

#### 3.1. Rainfall patterns statistic

The Wolong County belongs to the climate zone of Qinghai-Tibet plateau, whose weather is controlled by south branch of the westerly jet stream and the southeast monsoon. The weather of this area is dry and sunny with less rainfall in winter; while in the summer half year, under the influence of humid southeast monsoon, the rainfall of this area is abundant. Table 1 shows the years for which rain fall data were collected from 3 stations during the period June to September. They were used for statistical analyses.

**Table 1.** Periods in for which rainfall data were collected from the website <https://rp5.ru>

Station	WMO_ID	Location	Altitude	Monitoring Time
Dujiangyan	56187	30°42'N, 103°49.98'E	545m	01.01.2013~06.28.2018
Mianyang	56196	31°28'N, 104°41'E	522m	01.01.2013~06.28.2018
Ya'an	56287	29°59'N, 103°00'N	629m	01.01.2013~06.28.2018

The basic data was the hourly rainfall intensity which was calculated from the cumulative rainfall over time. A series of sequential data obtained from the stations which was divided into independent rainfall events, using two definitions: inter-event time definition and the effective rainfall definition [18,27]. An effective rainfall standard for a rainfall event was amended for Wenchuan earthquake area [28].

Based on the dimensionless rainfall-duration curve, standardized rainfall profiles (SRP) and Huff curves, the Binary Shape Code (BSC) was established and applied to Calabria (south Italy) to investigate the seasonality of erosivity [29,30]. 165 valid rainfall events have been chosen from the rainfall data in this paper, the rainfall events were divided into 4 categories of precipitation process to ensure that the properties of each category were similar, according to the clustering method of dynamic K-value proposed by Yin et al (2014) [31].

The rainfall pattern was one of the factors influencing the critical discharge of catchment, while precipitation evidently affected the critical discharge as well.

### 3.2. Hydrological analysis

The subbasins results of Xiongmao gully were obtained using Hydrology Model with ARCGIS10.1. It was found that the obtained subbasins were accurate when the cumulative grid number was 660; further, the above results were applied into HEC-HMS (Figure 6), and the watershed model was built by arranging subbasins, junctions, reach and sink, etc.

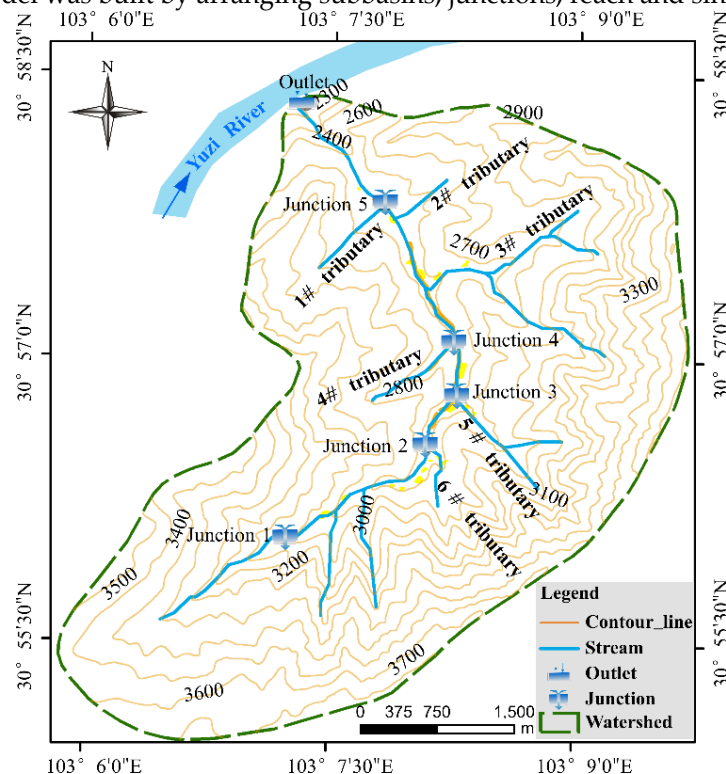


Figure 6. Distribution of junction in Xiongmao catchment

The input settings in HEC-HMS hydrological model contains infiltration property, initial soil water content and maximum saturate rainfall intensity, which values as 6% and 14mm in field test respectively.

Soil Conservation Service Curve (SCS) was adopted considering the impact of soil property, land use and soil moisture content at earlier stage on runoff generation and flow concentration. The Regional value depending on geographical and climatic factors was selected as 0.1-0.3 [32]; and it was normally 0.2 in semi-distributed hydrological model for precisely predicting the runoff [33,34], Curve Number (CN) and CN value [35,36] was 85 based on the practice soil type and vegetation cover in this studied area.

SCS Unit Hydrograph Transform taken as the transform method was used to calculate the peak discharge of unit hydrograph according to precipitation, catchment area, peak and confluence time [37]. The lag time combined with the longitudinal grade, runoff length, etc., of the catchment which were obtained from ARCGIS. Additionally, lag time parameter could be calculated by Lag Routing Method and Kinematic Wave Routing [38].

### 3.3. Hydrological analysis

Based on the water volume ( $Q_p$ , m<sup>3</sup>/s) at Junction 3 obtained from HEC-HMS, we used the modified flood method [17] considering the volumetric concentration of the solids ( $C_v$ , dimensionless) and blocking coefficient ( $D_c$ , dimensionless) to calculate the debris flow discharge ( $Q_c$ , m<sup>3</sup>/s),

$$Q_c = D_c Q_p / (1 - C_v), \quad (1)$$

In which,  $C_v$  represented the solid volume in a unit volume of debris flow, was calculated by Equation (2),

$$C_v = (\gamma - \gamma_w) / (\gamma_s - \gamma_w), \quad (2)$$

There were colluvium and decayed tree at the upper catchment of B-B' after field survey and the coefficient in this paper was set as 1.5. In Equation (2),  $C_v$  is the volume concentration of debris flow;  $\gamma$  the debris flow specific weight;  $\gamma_w$ , the specific weight of water ( $0.98 \times 10^3 \text{ kg/m}^3$ );  $\gamma_s$ , the solid specific weight ( $2.65 \times 10^3 \text{ kg/m}^3$ ).

In order to calculate the specific weight we used the Equation of Yu (2011)[39]: Coarse particles whose sizes were more than 20mm were removed from depositions of gullies to calculate debris flow concentration by grain grading analysis, as shown in Equation (3)

$$\gamma = P_{0.5}^{0.35} P_2 \gamma_v + \gamma_0, \quad (3)$$

in which  $\gamma$  is debris flow concentration (kg/m<sup>3</sup>);  $P_{0.5}$  the ratio of fine particles whose sizes were less than 0.05mm;  $P_2$  the ratio of coarse particles whose sizes were more than 2mm;  $\gamma_v$  the minimum concentration of viscous debris flow, equal to 20KN/m<sup>3</sup>; while  $\gamma_0$ , the minimum concentration of debris flow, is  $1.5 \times 10^3 \text{ kg/m}^3$ .

### 3.3. Critical debris flow discharge on flume test

Through a series of laboratory flume experiment, Wang et al (2017) [9] revealed the relationship between grain size distribution and the hydrodynamic conditions of debris flow. Based on the deposit characteristic of wide grading in the earthquake area of Wenchuan, the grain size of 0-60mm was selected, and the result was as follows:

$$q_c = 0.32 d_{84}^{2.5} / (\tan^2 \theta d_{16} C_u C_c^{0.4}), \quad (4)$$

For  $C_u = d_{60}/d_{10}$ , and  $C_c = d_{30}^2 / (d_{60} * d_{10})$ ,  $d_i$  was diameter corresponding to  $i\%$  cumulative distribution of particles smaller than the size; And  $d_{84}$  was the typical grain size of course particles, on the contrary,  $d_{16}$  was that of fine particles.

## 4. Results

Considering the abundant solid material on the channel bed initiate mainly, by contrast, the soil erosion of talus material along channel bank increased the concentration gently. Thus set the position of Junction 3 as monitoring cross section typically.

#### 4.1. Rainfall patterns

Figure 7 shows that the period during which the cumulative rainfall increased fastest was in the first period between 0% and 25% of the rainfall duration for Pattern-I and Pattern-II. They were defined as first-quartile rainfall according to the Huff curve. Considering the fact that debris flows broke out in most cases in the middle and later periods of a heavy rain events, Pattern-III with durations from 0%~50% of the total duration was regarded as the second-quartile rainfall; and Pattern-IV was classified in the same category as Pattern-III because the rainfall was concentrated in the duration period from 25%~50%.

Through statistical analyses on the rainfall data in the study over the years, the first-quartile and second-quartile rainfall of Pattern-I, -II, -III, -IV were applied in the Xiongmao gully, in order to reveal the hydrological response characteristics under typical rainfall conditions.

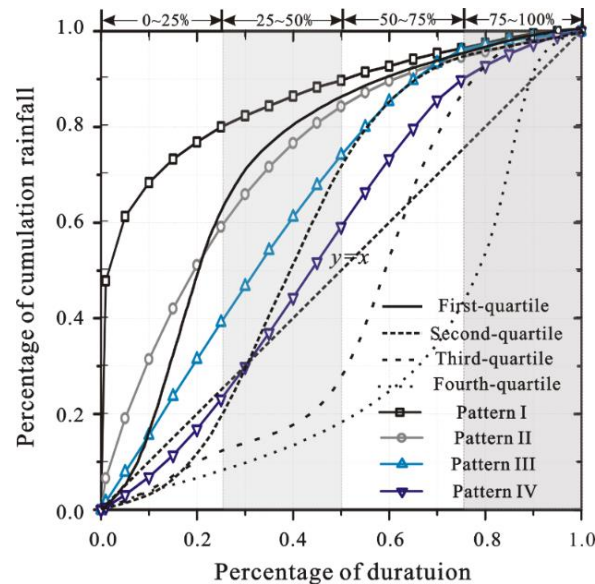


**Figure 7.** Typical curve of cumulative rainfall duration; and first-quartile, second-quartile, third-quartile, fourth-quartile stood for 50% probability level for Huff curve, corresponding to four kinds of curves in K-value clustering analysis on the data from the observation stations

As mentioned above, the rainfall intensities within 24h with frequencies of 100a, 50a, 20a, 10a in the Xiongmao gully were 211.5mm, 190.8mm, 162.0mm, and 139.5mm, respectively. The cumulative rainfall curves of Pattern I, Pattern II, Pattern III, Pattern IV were tends towards  $y=x$  graph gradually in Figure 7, i.e., and the rainfall intensity concentration degree decreases successively. The equations for the accumulated rainfall ( $R_a$ ) vs. duration ( $t$ ) for 4 types of rainfall patterns was acquired by K-value clustering analysis:

$$\text{Pattern I, } R_a = 0.1219\ln(t) + 0.9879, \quad R^2 = 0.9815$$

$$\text{Pattern II, } R_a = 1.7402t^3 - 3.984t^2 + 3.2591t, \quad R^2 = 0.9978$$

$$\text{Pattern III, } R_a = -0.7667t^3 + 0.1624t^2 + 1.5868t, \quad R^2 = 0.9996$$

$$\text{Pattern IV, } R_a = -1.8049t^3 + 2.3173t^2 + 0.4719t, \quad R^2 = 0.9997$$

#### 4.2. Runoff discharge for various rainfall patterns and frequencies

The rainfall intensity at any period could be calculated according to the above equations. The precipitation for a certain period and the distribution diagram of hourly rainfall intensity is presented in the upper part of Figure 8 for varying recurrent periods. Additionally, the hourly rainfall intensity distributions for different rainfall patterns were distinguished by different colors, corresponding to the discharge hydrograph of the confluence of Junction 2, 3 in Figure 6. To present the whole discharge process of a valid rainfall event, the time period was set within 48h.

Compared with the water volume curve in Xiongmao gully, the lower part of Figure 8, shows hydrographs at different junctions for different rainfall return periods and rainfall patterns. The rainfall frequencies influence the flow volumes, and it was found that the peak discharge was influenced by the rainfall patterns. The time at which the peak flows of Pattern I, II, III, and IV emerged are after 480~510min, 780~810min, 1080~1110min, and 1410~1470min, respectively. However, in Figure 8d, the peak flow for a frequency of 10a appeared a little later and lasted for a longer time, indicating that the storage capacity of the vegetation and soil in the catchment retarded and decreased the peak flow.

Pattern I shows larger peak flows at rainfall frequencies of 100a and 50a, because the high intensity rains for this Pattern causes high runoff. The peak flows of Pattern I with the rainfall frequencies of 20a and 10a, are more or less equal to the peaks for the other patterns with the same frequencies or even less than the runoff peaks of Pattern IV. It means that larger peaks more likely appears in uniform rainfall patterns.

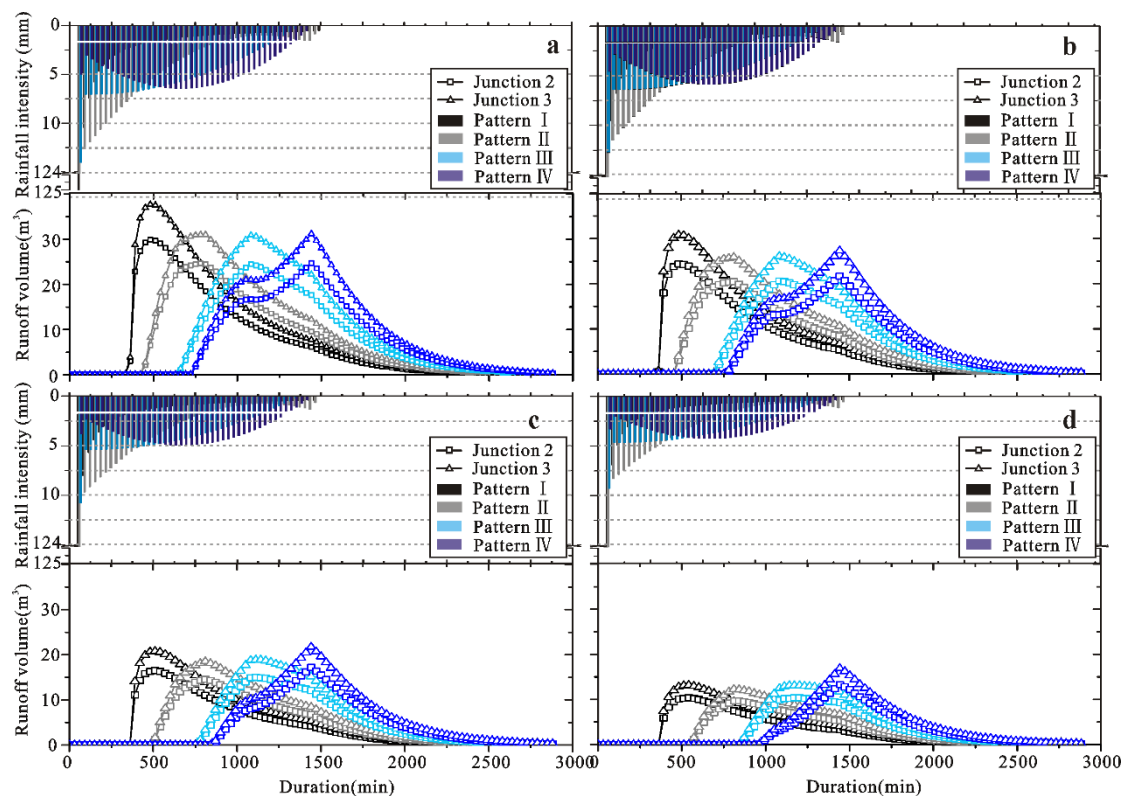


**Figure 8.** Runoff volume at different junctions. (a),(b),(c) and (d) depict the rainfall intensity (upper) and runoff volume (lower) at the frequencies of 100a, 50a, 20a, 10a in Xiongmao gully

#### 4.3. Discharge of debris flow and threshold on July, 26<sup>th</sup>

Samples were taken from debris flow deposits and colluvial material at a depth of 0-50 cm for the particle grading test; then grading curve were acquired from laboratory analyses and grading on particle samples less than 2mm. (Figure 9)

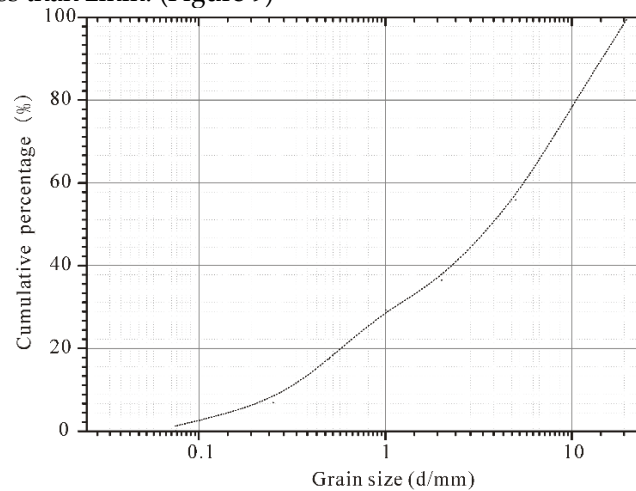


**Figure 9.** Grading curve of the debris flow deposits in Xiongmao Gully, and the corresponding location shown in Figure 2.

The investigated section of the debris flow in Xiongmao gully, B-B',  $d_{10}=0.45\text{mm}$ ,  $d_{16}=0.8\text{mm}$ ,  $d_{30}=1.24\text{mm}$ ,  $d_{60}=18\text{mm}$ ,  $d_{84}=36\text{mm}$ ,  $\tan\theta=0.063$ ; then the critical unit discharge of B-B' was  $q_c=1.206\text{m}^3/\text{s}\cdot\text{m}$ , and the critical discharge was  $Q_c=43.8\text{m}^3/\text{s}$ .

Referring to Figure 9, the granular size test point of Test 4, valued  $P_{0.05}$  and  $P_2$  as Table 2, and calculated by equation (2) and equation (3), the debris flow density is  $\gamma_D=1.67\times 10^3\text{kg}/\text{m}^3$ , the volumetric concentration of the solids  $C_v=0.42$ . The field survey indicated that the maximum flow of debris flow, on July, 26<sup>th</sup>, 2016, was  $Q_c=66.7\text{m}^3/\text{s}$ . Table 2 was shown below calculated by Figure 9 and equation (3).

**Table 2.** Debris flow parameters at different points of Xiongmao Gully

Test location	$P_{0.05}$	$P_2$	$\gamma_D$	$C_v$
Sample test 4	1.3%	63.5%	1.67	0.42

As indicated in critical discharge analysis, the rainfall conditions could lead to the outbreak of the debris flow on July, 26<sup>th</sup>, 2016; except for the catchment topography, source distribution, the prediction on the rainfall condition under which debris flow could happen was the aim of this study. Calculate with Equation (1) and Equation (2), the debris flow discharges at cross section B-B' under rainfall conditions at a frequency of 10a, 20a are shown in Figure 10, and it can be seen that debris flow hardly happened in Xiongmao gully at the frequency of 10a; while debris flow was more likely to happen under 4 rainfall patterns at the frequency of 20a.

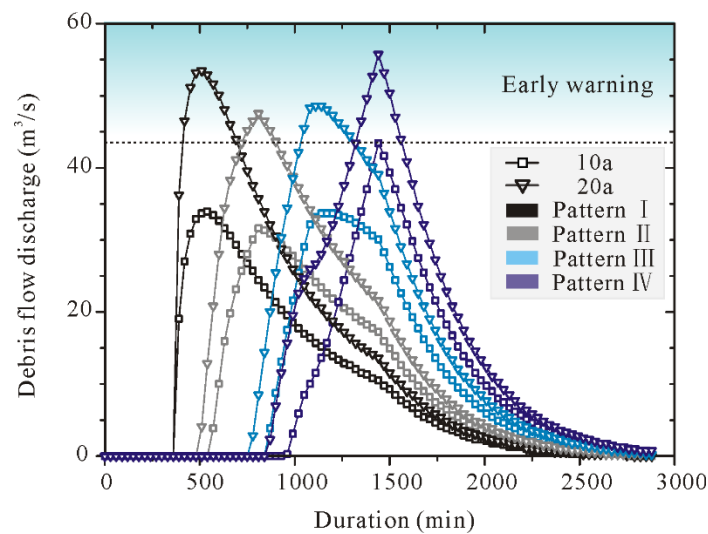


**Figure 10.** Discharge (under consideration of blocking while  $D_c = 1.5$ ) of B-B' under the conditions of different rainfall patterns, square was the debris flow discharge induced by rainfall at the frequency of 10a; Inverted triangle was the debris flow discharge induced by rainfall at the frequency of 20a; dash dot line was the critical discharge on B-B'.

The dash dotted lines in Figure 10 are the critical discharges at B-B', corresponding to Junction 2 and 3. It shows 4 possible rainfall patterns leading to debris flow at the B-B' cross section and that critical precipitation and duration are varying for different rainfall patterns. The rainfall threshold has a maximum at 1h, and 6h for Pattern I; while it is the lowest for Pattern IV.

## 5. Discussion

As shown in Figure 10, the peak discharge and time are effected on various rainfall patterns and frequency. In addition, the input parameters in HEC-HMS have great influence on simulated response, so the sensitivity analysis should be take consideration. Some confuse emerge on the debris flow discharge based on the Equation (1), which is the uncertainly on valuing on  $D_c$  in particular. The main topics discussed on debris flow discharge include rainfall patterns, parameters, and uncertain valuing.

### 5.1. Statistical rainfall patterns

Huff (1967) [22] quartered the curve into first-quartile, second-quartile, third-quartile, and fourth-quartile, and further, dimensionless curve was depicted by dividing into 9 probability levels from 10%, 20%...till to 90%. According to the above listed rainfall data and K value clustering analysis, 4 patterns, cumulative percentage-duration percentage, were categorized as shown in Figure 11. Most of studies on the median curve is the typical curve, and 50% probability level was the most suitable for the simulation on runoff discharge in practice. Figure 11 depicted Huff curve of 50% probability level stressed by the varying dot dash lines.

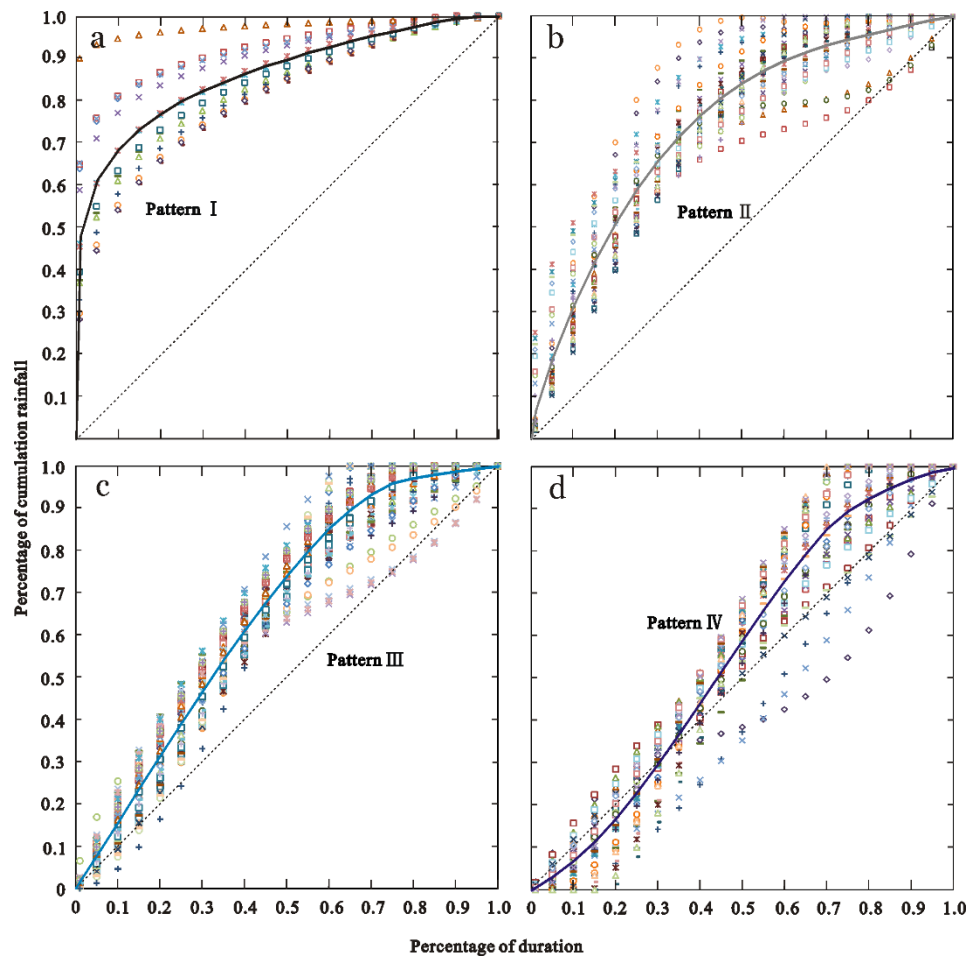


**Figure 11.** the scatter diagram of rainfall patterns. 4 kinds of rainfall patterns including Pattern I, Pattern II, Pattern III, Pattern IV according to K value clustering analysis

For all the 165 rainfall events, 14 events belong to Pattern I (8.48 %); 40 events to Pattern-II (24.24%); 71 events to Pattern-III (43.03%); and the rest to Pattern-IV of (24.24%). The antecedent precipitation dominates in Pattern-I. The research results revealed that Pattern-I tended to a temporal rainfall duration less than 12h in general. Pattern-II represents rainstorms of temporal rainfall as well.

Zhou et al (2014) [19] pointed out that the rainfall thresholds varies between 7.8~38.4mm/h for debris flows which occurred in the earthquake area of Wenchuan. For many rainfall events, different rainfall patterns result to various discharge and previous water content. Compared with Table 3, the rainfall threshold of the critical discharge of debris flow was varying with rainfall patterns, and the maximum hourly rainfall intensities of Pattern II, Pattern III, and Pattern IV at earlier stage were consistent with the results of pre-study. While the maximum hourly rainfall intensity was 97.3mm/h for Pattern I, the abrupt heavy rain mode. It can be known from the maximum rainfall threshold at earlier stage of 1h 6h that antecedent precipitation made the threshold value decrease compared with the heavy rainfall at short duration (Pattern I).

**Table 3.** The rainfall threshold at the time of critical discharge on C-C'

Rainfall pattern	time /min	maximum precipitation at earlier stage /mm	
		1h	6h
Pattern I	410	97.3	132.7
Pattern II	720	20.9	96.1
Pattern III	1010	10.7	64
Pattern IV	1320	9.9	53.5

### 5.2. Parameters sensitivity analysis of HEC-HMS

For the hydrograph discharge, sampling test have ensure the value accuracy such as initial storage, maximum surface storage, and CN values, geographical and climatic factors, potential maximum retention, maximum vegetation interception proposed in the literature [32,34,36,40]. Based on the method of sensitivity analysis [13], the sensitivity of HEC-HMS simulated flow discharge with 4 parameters, as Table 4.

**Table 4.** Parameters sensibility analysis for HEC-HMS simulations of hydrological response

Parameters	The change ratio of peak flow after a certain proportion of single increase/decrease		
	The basic condition	Increase by 10%	Lower by 10%
CN	85	0.28	-0.16
Vegetation interception	13mm	-0.2	2
Initial storage	6%	0.01	-0.01
Surface storage	14mm	-0.02	0.02

It can be concluded that, changing with the increasing/decreasing parameters from the simulations, the results simulated as different percentage of discharge relative the base case. Which shown that the CN value plus 10% or minus 10% led to 28% increase and 16% lower of peak discharge. The valuing on CN has a significant influence on flow discharge and other parameters has a weak influence on Xiongmao gully.

### 5.3. Valuing on debris flow discharge

For the debris flow discharge,  $Q_p$  and  $C_v$  were known in settings contain particle size and specific weight of debris flow or water, then we choose the Equation (1) avoiding more parameters except  $D_c$ . The  $D_c$ , valued with the blocking degree of channel, has a great influence on discharge. The lowest early warning area when neglect channel blocking (while  $D_c = 1.0$ ) was shown in Figure 12. Compared with Figure 10 ( $D_c = 1.5$ ), which considering the slight blocking. Choosing the C-C' as the analytic crossing section for observably initiation, which could reduce influence on predicting result for various  $D_c$ . All the patterns of 50a rainfall frequency will lead to sediment initiation while discharge may increase along channel in reality. And compared with the frequency of 20a, shorter durations of 50a frequency generate larger runoff in Xiongmao catchment.

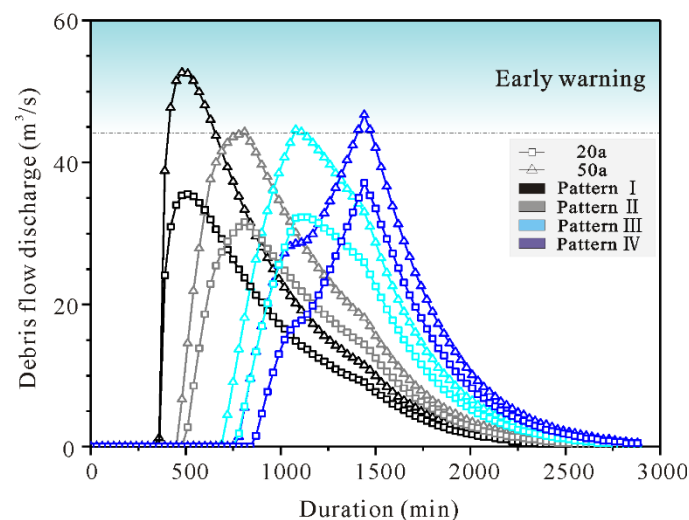


**Figure 12.** Discharge (no consideration of blocking while  $D_c = 1.0$ ) of B-B' under the conditions of different rainfall patterns, square was the debris flow discharge induced by rainfall at the frequency of 10a; Inverted triangle was the debris flow discharge induced by rainfall at the frequency of 20a; dash dot line was the critical discharge on B-B'.

## 6. Conclusions

It was indicated by field survey that the outbreak of the 2016 debris flow in the Xiongmao gully was due to rainfall runoff flooding and erosion of earlier alluvial deposits along the channel banks and channel bed. Laboratory test relation has used to calculate the debris flow discharge on July, 26<sup>th</sup>, 2016, which is lower than the discharge on field survey. Based on the analyses presented above, the following conclusions may be presented:

The increasing concentration of runoff and abundant channel sediment made the debris flow occurrence. The gentle gradient and straight channel on upstream and midstream ensured that debris flow on Xiongmao gully grow slightly with increasing concentration and discharge. With a return period of 50a, deposition initiated in the wide middle of the stream primitively.

The critical discharge at the B-B' cross section is 43.78 m<sup>3</sup>/s, which is lower than the morphological survey of the debris flow delivered a critical discharge of  $Q_c=66.7\text{m}^3/\text{s}$  (at the frequency of 50a).

The K-value clustering analysis of the precipitation revealed that there were 4 rainfall patterns. Pattern-I and pattern-II are the cumulative rainfall grew fastest in the duration 0% to 25%, characterized by heavy rainfall with short duration, which counted for 32.7%; the duration period in which rainfall was concentrated most is between 25%-50% for Pattern-III and Pattern-IV, weighting at 67.3%.

Debris flow was more likely to occur under 4 rainfall patterns at the frequency of 20a in Xiongmao gully, but with the debris material decrease upstream, the rainfall frequency of 50a would be needed.

**Author Contributions:** Conceptualization, L.F.G. and C.T.; methodology, L.F.G. and J.X.; validation, L.F.G., C.T., J.X. and N.L.; formal analysis, L.F.G.; investigation, L.F.G., J.X. and N.L.; resources, C.T.; data curation, J.X.; writing—original draft preparation, L.F.G.; writing—review and editing, C.T.; visualization, L.F.G.; supervision, C.T.; project administration, C.T.; funding acquisition, C.T. All authors have read and agreed to the published version of the manuscript.

**Funding:** This research was funded by the National Natural Science Foundation of China, grant number 41672299 and the National Key Research and Development Program of China, grant number 2017YFC1501004.

**Acknowledgments:** Prof. Theo van Asch helped to improve the language, and his suggestion of the paper is gratefully acknowledged, and the Huadi Construction Engineering Limited Company of Sichuan is gratefully acknowledged for precious pictures. The authors thank the anonymous reviewers for their helpful suggestions to improve the paper.

**Conflicts of Interest:** The authors declare no conflict of interest.

## References

1. Coe, J.A.; Glancy, P.A.; Whitney, J.W. Volumetric analysis and hydrologic characterization of a modern debris flow near Yucca Mountain, Nevada. *Geomorphology* **1997**, *20*, 11-28, doi:https://doi.org/10.1016/S0169-555X(97)00008-1.
2. Coe, J.A.; Kinner, D.A.; Godt, J.W. Initiation conditions for debris flows generated by runoff at Chalk Cliffs, central Colorado. *Geomorphology* **2008**, *96*, 270-297, doi:10.1016/j.geomorph.2007.03.017.
3. Godt, J.W.; Coe, J.A. Alpine debris flows triggered by a 28 July 1999 thunderstorm in the central Front Range, Colorado. *Geomorphology* **2007**, *84*, 80-97, doi:https://doi.org/10.1016/j.geomorph.2006.07.009.
4. Takahashi, T. Mechanical characteristics of debris flow. *ASCE J Hydraul Div* **1978**, *104*, 1153-1169.
5. Gregoretti, C. The initiation of debris flow at high slopes: experimental results. *Journal of Hydraulic Research* **2010**, *38*, 83-88, doi:10.1080/00221680009498343.
6. Gregoretti, C.; Fontana, G.D. The triggering of debris flow due to channel-bed failure in some alpine headwater basins of the Dolomites: analyses of critical runoff. *Hydrological Processes* **2008**, *22*, 2248-2263, doi:10.1002/hyp.6821.

7. C, T.; GR, B.; HE, M. Threshold criterion for debris-flow initiation due to channel-bed failure. In Proceedings of Proceeding of the 2nd international conference on debris flow, hazards and mitigation, Taipei; pp. 89-97.
8. Lyu, L.; Wang, Z.; Cui, P.; Xu, M. The role of bank erosion on the initiation and motion of gully debris flows. *Geomorphology* **2017**, *285*, 137-151, doi:10.1016/j.geomorph.2017.02.008.
9. Wang, Y.; Cui, P.; Wang, Z.; Liang, S. Threshold criterion for debris flow initiation in seasonal gullies. *International Journal of Sediment Research* **2017**, *32*, 231-239, doi:10.1016/j.ijsrc.2017.03.003.
10. Tang, C.; Zhang, S.C. Study progress and expectation for initiation mechanism and prediction of hydraulic-drive debris flows. *Advances in Earth Science* **2008**, *23*, 787-793.
11. Van Asch, T.; Yu, B.; Hu, W. The Development of a 1-D Integrated Hydro-Mechanical Model Based on Flume Tests to Unravel Different Hydrological Triggering Processes of Debris Flows. *Water* **2018**, *10*.
12. Collischonn, W.; Haas, R.; Andreolli, I.; Tucci, C.E.M. Forecasting River Uruguay flow using rainfall forecasts from a regional weather-prediction model. *Journal of Hydrology* **2005**, *305*, 87-98, doi:10.1016/j.jhydrol.2004.08.028.
13. Ran, Q.-h.; Qian, Q.; Li, W.; Fu, X.-d.; Yu, X.; Xu, Y.-p. Impact of earthquake-induced-landslides on hydrologic response of a steep mountainous catchment: a case study of the Wenchuan earthquake zone. *Journal of Zhejiang University-SCIENCE A* **2015**, *16*, 131-142, doi:10.1631/jzus.A1400039.
14. Rickenmann, D. Empirical relationships for debris flows. *Nat Hazards* **1999**, *19*, 47-77, doi:10.1023/A:1008064220727.
15. Chen, N.S.; Yue, Z.Q.; Cui, P.; Li, Z.L. A rational method for estimating maximum discharge of a landslide-induced debris flow: A case study from southwestern China. *Geomorphology* **2007**, *84*, 44-58, doi:https://doi.org/10.1016/j.geomorph.2006.07.007.
16. Cui, P.; Zhou, G.G.D.; Zhu, X.H.; Zhang, J.Q. Scale amplification of natural debris flows caused by cascading landslide dam failures. *Geomorphology* **2013**, *182*, 173-189, doi:10.1016/j.geomorph.2012.11.009.
17. Shen, S.; Xie, X.; Xiang, X.; Li, L.; Gong, C.; Bai, Y.; Xie, X. On Estimation of Debris Flow Discharges. *China Railway Science* **1993**.
18. Jan, C.-D.; Lee, M.H. A debris-flow rainfall-based warning model. *Journal of Chinese Soil and Water Conservation* **2004**, *35*, 275-285.
19. Zhou, W.; Tang, C.; Van Asch, T.W.J.; Zhou, C. Rainfall-triggering response patterns of post-seismic debris flows in the Wenchuan earthquake area. *Natural Hazards* **2014**, *70*, 1417-1435, doi:10.1007/s11069-013-0883-8.
20. Guo, X.; Cui, P.; Li, Y.; Ma, L.; Ge, Y.; Mahoney, W.B. Intensity-duration threshold of rainfall-triggered debris flows in the Wenchuan Earthquake affected area, China. *Geomorphology* **2016**, *253*, 208-216, doi:https://doi.org/10.1016/j.geomorph.2015.10.009.
21. Dunkerley, D. Effects of rainfall intensity fluctuations on infiltration and runoff: rainfall simulation on dryland soils, Fowlers Gap, Australia. *Hydrological Processes* **2012**, *26*, 2211-2224, doi:10.1002/hyp.8317.
22. Huff, F.A. Time distribution of rainfall in heavy storms. *Water Resources Research* **1967**, *3*, 1007-1019, doi:10.1029/WR003i004p01007.
23. Huff, F.A. *Time distributions of heavy rainstorms in illinois*; Illinois State Water Survey: 1990; pp 1007-1012.
24. Bonnin, G.M.; Martin, D.; Lin, B.; Parzybok, T.; Yekta, M.; Riley, D.; Brewer, D.; Hiner, L. Updates to NOAA Precipitation Frequency Atlases. **2007**, 10.1061/40927(243)413, 1-10, doi:10.1061/40927(243)413.
25. Azli, M.; Rao, A.R. Development of Huff curves for Peninsular Malaysia. *Journal of Hydrology* **2010**, *388*, 77-84, doi:10.1016/j.jhydrol.2010.04.030.
26. Dolšak, D.; Bezak, N.; Šraj, M. Temporal characteristics of rainfall events under three climate types in Slovenia. *Journal of Hydrology* **2016**, *541*, 1395-1405, doi:10.1016/j.jhydrol.2016.08.047.
27. Molina-Sanchis, I.; Lázaro, R.; Arnau-Rosalén, E.; Calvo-Cases, A. Rainfall timing and runoff: The influence of the criterion for rain event separation. *Journal of Hydrology and Hydromechanics* **2016**, *64*, 226-236, doi:10.1515/johh-2016-0024.
28. Zhou, W.; Tang, C.; Van Asch, T.W.J.; Chang, M. A rapid method to identify the potential of debris flow development induced by rainfall in the catchments of the Wenchuan earthquake area. *Landslides* **2015**, *13*, 1243-1259, doi:10.1007/s10346-015-0631-0.
29. Terranova, O.G.; Iaquina, P. Temporal properties of rainfall events in Calabria (southern Italy). *Natural Hazards and Earth System Science* **2011**, *11*, 751-757, doi:10.5194/nhess-11-751-2011.

30. Terranova, O.; Gariano, S.L. Rainstorms able to induce flash floods in a Mediterranean-climate region (Calabria, southern Italy). *Natural Hazards and Earth System Sciences* **2014**, *14*, 2423-2434, doi:10.5194/nhess-14-2423-2014.
31. Yin, S.; Wang, Y.; Xie, Y.; Liu, A. Characteristics of intra-storm temporal pattern over China. *Advances in Water Science* **2014**, *25*, 617-624.
32. Patil, J.P.; Sarangi, A.; Singh, A.K.; Ahmad, T. Evaluation of modified CN methods for watershed runoff estimation using a GIS-based interface. *Biosystems Engineering* **2008**, *100*, 137-146, doi:https://doi.org/10.1016/j.biosystemseng.2008.02.001.
33. Mishra, S.; Singh, V.; Sansalone, J.; Aravamuthan, V. A modified SCS-CN method: Characterization and testing. *Water Resources Management* **2003**, *17*, 37-68, doi:10.1023/A:1023099005944.
34. Mishra, S.K.; Singh, V.P. Long-term hydrological simulation based on the Soil Conservation Service curve number. *Hydrological Processes* **2004**, *18*, 1291-1313, doi:10.1002/hyp.1344.
35. USDA. Soil conservation service national engineering handbook. us, 1993.
36. FU, S.; WANG, X.; WANG, H.; WEI, X.; YUAN, A. Method of determining CN value in the SCS-CN method. *Arid Land Geography* **2012**, *35*, 415-421.
37. Zhao, J.; Huang, Q.; Hao, P.; Tian, W. Research on Flood Real-Time Forecasting Based on SCS Model. *Journal of Xi'an University of Technology* **2013**, *29*, 386-391.
38. Xie, P.; Ye, S. The research on parameters relationship among of the methods channel flood routing. *International Journal Hydroelectric Energy* **1993**, *10*, 242-247.
39. Yu, B. Research on prediction of debris flows triggered in channels. *Natural Hazards* **2011**, *58*, 391-406, doi:10.1007/s11069-010-9673-8.
40. Miao, R. *Physical Hydrology*; Water Resources and Electric Power Press: Baijing, 2007.